THE JOURNAL OF COMPARATIVE NEUROLOGY 385:245–264 (1997)

Projections From the Ventral Cochlear Nucleus to the Dorsal Cochlear Nucleus in Rats

JOHN R. DOUCET* AND DAVID K. RYUGO
Center for Hearing Sciences, Departments of Otolaryngology-Head and Neck Surgery and Neuroscience, Johns Hopkins University School of Medicine, Baltimore, Maryland 21205

ABSTRACT

Local circuit interactions between the dorsal and ventral divisions of the cochlear nucleus are known to influence the evoked responses of the resident neurons to sound. In the present study, we examined the projections of neurons in the ventral cochlear nucleus to the dorsal cochlear nucleus by using retrograde transport of biotinylated dextran amine injected into restricted but different regions of the dorsal cochlear nucleus. In all cases, we found retrogradely labeled granule, unipolar brush, and chestnut cells in the granule cell domain, and retrogradely labeled multipolar cells in the magnocellular core of the ventral cochlear nucleus. A small number of the labeled multipolar cells were found along the margins of the ventral cochlear nucleus, usually near the boundaries of the granule cell domain. Spherical bushy, globular bushy, and octopus cells were not labeled. Retrogradely-labeled auditory nerve fibers and the majority of labeled multipolar neurons formed a narrow sheet extending across the medial-to-lateral extent of the ventral cochlear nucleus whose dorsoventral position was topographically related to the injection site. Labeled multipolar cells within the core of the ventral cochlear nucleus could be divided into at least two distinct groups. Planar neurons were most numerous, their somata found within the associated band of labeled fibers, and their dendrites oriented within this band. This arrangement mimics the organization of isofrequency contours and implies that planar neurons respond best to a narrow range of frequencies. In contrast, radiate neurons were infrequent, found scattered throughout the ventral cochlear nucleus, and had long dendrites oriented perpendicular to the isofrequency contours. This dendritic orientation suggests that radiate neurons are sensitive to a broad range of frequencies. These structural differences between planar and radiate neurons suggest that they subserve separate functions in acoustic processing. J. Comp. Neurol. 385:245–264, 1997.

Indexing terms: auditory system; biotinylated dextran amine; hearing; neuroanatomy; tonotopy

The cochlear nucleus may be considered the gateway to the central auditory system, receiving and processing input from auditory nerve fibers and projecting its output along several parallel pathways to higher auditory nuclei. The cochlear nucleus traditionally is partitioned into three divisions, the dorsal cochlear nucleus (DCN), the posteroventral cochlear nucleus (PVCN), and the anteroventral cochlear nucleus (AVCN). In contrast to the relative homogeneity observed amongst myelinated auditory nerve fibers, each nuclear subdivision contains a diverse array of cell types that can differ in their morphology, physiology, projection patterns, and neurochemistry. This diversity is particularly prominent in the DCN (Brawer et al., 1974; Lorente de Nó, 1981; Hackney et al., 1990; Osen et al., 1990). The exact role of the DCN in acoustic processing is not known, but its projection neurons are exquisitely sensitive to peaks and valleys in the stimulus spectrum which are thought to be important features in sound encoding (e.g., Spirou and Young, 1991; Nelken and Young, 1994). In order to account for this sensitivity, a necessary step is a more complete description of the neurons that innervate the DCN.

The DCN receives a robust innervation from the ventral divisions of the cochlear nucleus (Lorente de Nó, 1933;

Grant sponsor: National Institute on Deafness and other Communication Disorders (NIH); Grant numbers: RO1 DC00232, P60 DC00979.

*Correspondence to: Dr. John R. Doucet, Johns Hopkins Univ. Sch. of Med., Center for Hearing Sciences, Traylor 510, 720 Rutland Avenue, Baltimore, MD 21205. E-mail: jdoucet@bme.jhu.edu

Received 13 November 1996; Revised 11 March 1997; Accepted 1 April 1997

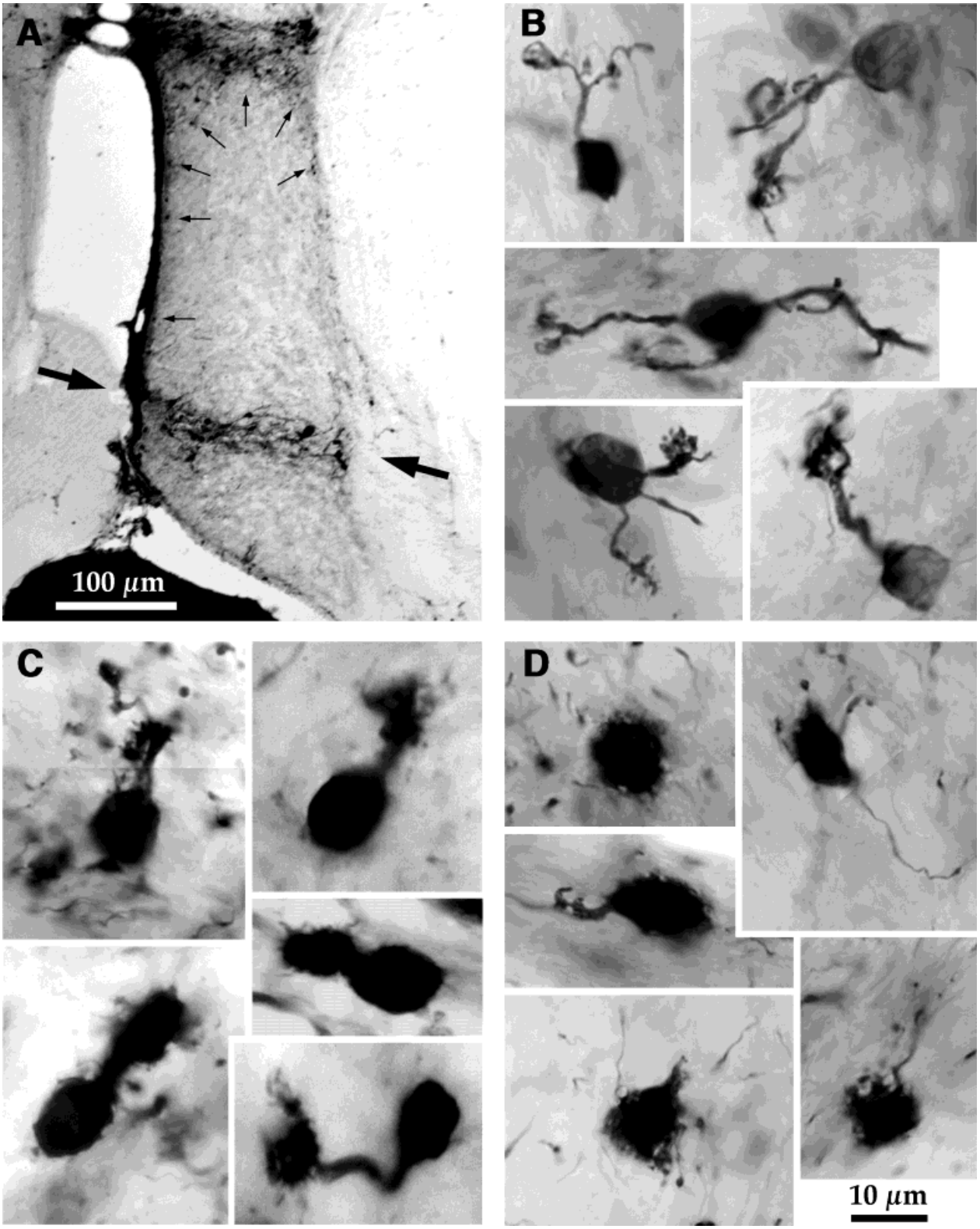

Fig. 1. **A:** Photomicrograph of a coronal section through the anterior ventral cochlear nucleus (AVCN) demonstrating the typical pattern of labeled cells after a biotinylated dextran amine (BDA)-injection is made into a restricted region of the dorsal cochlear nucleus (DCN). Notice that in the magnocellular core of the AVCN, the labeled cells and processes are confined to a band (denoted by large arrows) that runs across the medial-to-lateral extent of the nucleus. Surrounding the core, numerous labeled microneurons (some denoted by small arrows) are found in the granule cell domain. The labeled microneurons consist of at least three types. **B:** Granule cells are characterized by the claw-like structures terminating each of their dendritic branches. **C:** Unipolar brush cells are distinguished by having a single thick dendrite which ends in a spiral whorl of fine dendritic processes. **D:** Chestnut cells have no clearly-definable dendrites, but exhibit many short finger-like processes emanating from the cell body.

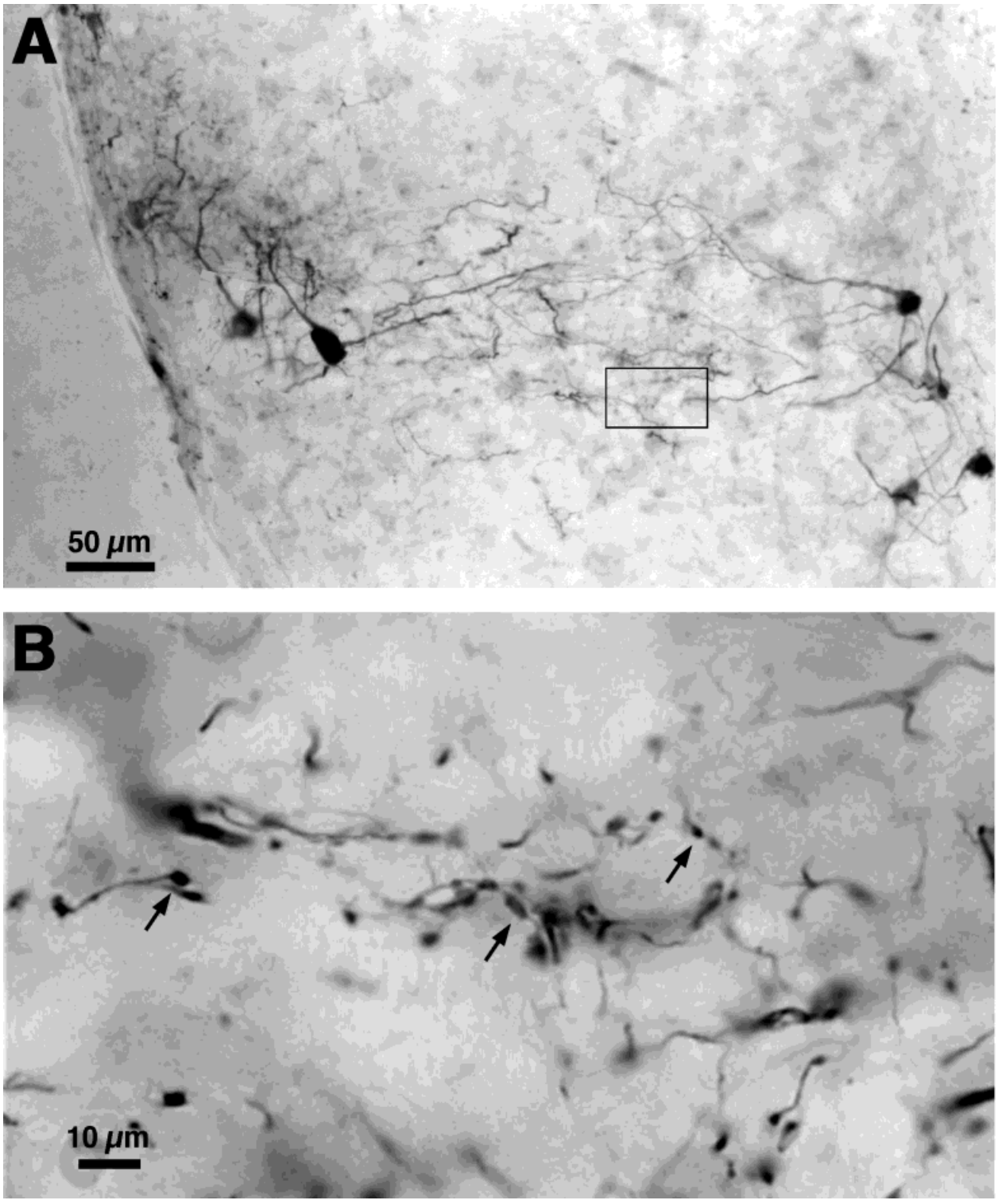

Fig. 2. Photomicrographs of the band of labeling in the ventral cochlear nucleus (VCN). **A:** This photomontage illustrates that the band is composed of BDA-filled cell bodies and dendrites, along with pieces of dendrites and/or axons associated with cells lying in nearby sections. Notice also that the path of the labeled dendrites and axons is confined to the band. The box denotes the region viewed at higher magnification in (B). **B:** This micrograph shows that labeled axons collectively give rise to numerous terminals (a few denoted by arrows). One source for these terminals is almost certainly retrogradely-filled auditory nerve fibers, suggesting that labeled VCN cells in the band and the region of the DCN they innervate are contacted by the same auditory nerve fibers.

Warr, 1966). Prior studies have indicated that multipolar cells of the ventral cochlear nucleus (VCN) convey the bulk of this projection to the DCN (Kane and Finn, 1977; Lorente de Nó, 1981; Adams, 1983; Feng and Vater, 1985; Snyder and Leake, 1988). One hypothesized role for this projection is that DCN neurons seem to be inhibited by a broadly-tuned input from some as yet unknown source, and the physiological class of onset choppers found in the VCN is suspected to be the source of this inhibitory input (Palmer and Winter, 1993; Nelken and Young, 1995).

There are two general classes of multipolar (or stellate) cells in the VCN that have been demonstrated to project to the DCN. Onset choppers, one class of VCN multipolar neuron, are found to have regular interspike intervals at stimulus onset, broad tuning, wide dynamic ranges (Smith and Rhode, 1989; Rhode and Greenberg, 1994; Winter and Palmer, 1995; Jiang et al., 1996; Palmer et al., 1996), and are correlated to the morphologic class of neurons exhibiting radiating dendrites and pleomorphic synaptic vesicles in their terminals (Smith and Rhode, 1989). Sustained choppers are another class of VCN multipolar neuron known to project to the DCN (Smith and Rhode, 1989). Sustained choppers have regular interspike intervals throughout a stimulus, sharp tuning, narrow dynamic ranges (Smith and Rhode, 1989; Rhode and Greenberg, 1994; Winter and Palmer, 1995; Jiang et al., 1996; Palmer et al., 1996), and are correlated with planar dendrites and round synaptic vesicles in their terminals (Smith and Rhode, 1989). Two very similar morphological classes of VCN multipolar neurons have been shown to project to the DCN in the mouse (Oertel, et al., 1990). Because the structure-function data are derived from the very difficult intracellular recording and staining methods of single neurons (Smith and Rhode, 1989; Oertel et al., 1990), the number of direct correlations are necessarily small. Thus, the global pattern of multipolar cell projections to the DCN has not been revealed.

In the present study, we examined the projections and types of VCN neurons in rats that project to the DCN by using the retrograde transport of biotinylated dextran amine (BDA). We made single extracellular injections of a 10% solution of BDA into restricted loci of the DCN. The injection site was varied systematically across different experiments so that collectively, the sites covered the entire DCN. This experimental strategy allowed us to analyze the spatial pattern of labeled cells in the VCN, to identify the cell type of origin of this projection, and to infer the nature of the terminal fields in the DCN.

MATERIALS AND METHODS

Surgical preparation

This study describes data derived from 10 male Sprague Dawley rats weighing between 250–400 g. All procedures were used in accordance with the guidelines and approval of the Animal Care and Use Committee of the Johns Hopkins Medical School. In each experiment, the rat was anesthetized with an intraperitoneal injection of Nembutal (40 mg/kg), and an intramuscular injection of atropine sulfate (0.1 cc) was given to reduce secretions. When the animal was areflexic to a paw pinch, the soft tissues overlying the dorsal aspect of the skull were cut and reflected, and an opening was drilled on one side of the occipital bone to expose the posterior aspect of the cerebellar cortex. A portion of the cerebellum extending from the vermis towards the flocculus was aspirated so that the entire DCN could be clearly viewed. An electrode (tip diameter, 10–20 µm) filled with a 10% (w/v) solution of biotinylated dextran amine (BDA, mw 10,000, Molecular Probes, Eugene, OR) in 0.01 M phosphate buffer (pH 7.4) was then aimed at the DCN and advanced with a hydraulic microdrive to a depth of 200 µm below the DCN surface. The application of positive current pulses (5 µA, 7 s on, 50% duty cycle, 3–5 minutes) was used to inject the BDA solution. Afterwards, the incision was sutured and the animal allowed to recover.

Histological processing

At least 24 hours after the injection, the animal was deeply anesthetized by the administration of a lethal dose of Nembutal and perfused with a solution of phosphate buffered saline (pH 7.4) with 0.1% $NaNO_2$ (causing vasodilation) followed immediately by a solution of 0.1 M phosphate buffer containing 0.1 M lysine, 0.01 M sodium periodate, and containing 4% paraformaldehyde (pH 7.4). The brainstem was dissected, allowed to postfix in the 4% paraformaldehyde solution for 1 hour at 21°C, embedded in a block of gelatin-albumin, and sectioned in the coronal plane using a Vibratome at a thickness of 50 µm. All sections through the cochlear nucleus were kept in serial order and incubated overnight at 4°C in a standard avidin biotin complex (ABC) solution (Vector Labs, Burlingame, CA). The following morning, sections were washed twice for 5 minutes each in phosphate buffer followed by two washes in 0.05 M cacodylate buffer (pH 7.2). Sections were incubated for 10 minutes in a Nickel/DAB solution consisting of 0.0125% 3,3′-diaminobenzidine (DAB), 0.25% nickel ammonium sulfate, and 0.35% imidazole in cacodylate buffer. Subsequently, hydrogen peroxide was added to the Nickel/DAB solution to yield a final hydrogen peroxide concentration of 0.02% and the sections were incubated for 15 more minutes. The sections were then washed twice with cacodylate buffer, followed by two washes with phosphate buffer. A few sections through the VCN containing darkly labeled cells were set aside for electron microscopic processing for a future study. The remaining sections were mounted on subbed slides, air-dried overnight, some were counterstained with cresyl violet, and all were coverslipped with Permount.

Data analysis

The reaction product in BDA-labeled cells appeared black when viewed with a light microscope. For all experi-

Fig. 3. Photomontages and corresponding drawing tube reconstructions of labeled radiate neurons. For each panel, a photomontage of the coronal section containing the radiate neuron cell body is shown on the left and the reconstructed radiate neuron is shown on the right. A photomontage was used to reconstruct the radiate neuron in (A) whereas a drawing tube was used to reconstruct the radiates in (B–D). The 100 µm scale bars refer to the coronal sections and the 25 µm scale bars refer to the reconstructed radiate neurons. Arrowheads denote the band of retrograde labeling in each section and the arrows point to the radiate neuron cell body. **A–C:** Examples of radiate neurons found in the AVCN, whereas (**D**) shows a radiate neuron located in the posteroventral cochlear nucleus (PVCN). Radiate neurons of the AVCN and PVCN were morphologically indistinguishable. One of the distinguishing features of radiate neurons is illustrated in panel C, where part of the granule cell domain (GCD) is indicated. The tips of radiate neuron dendrites could often be followed into the granule cell domain where they branched repeatedly. The reconstructions may not be complete because thick branches in several of the reconstructions end abruptly. D, dorsal; M, medial.

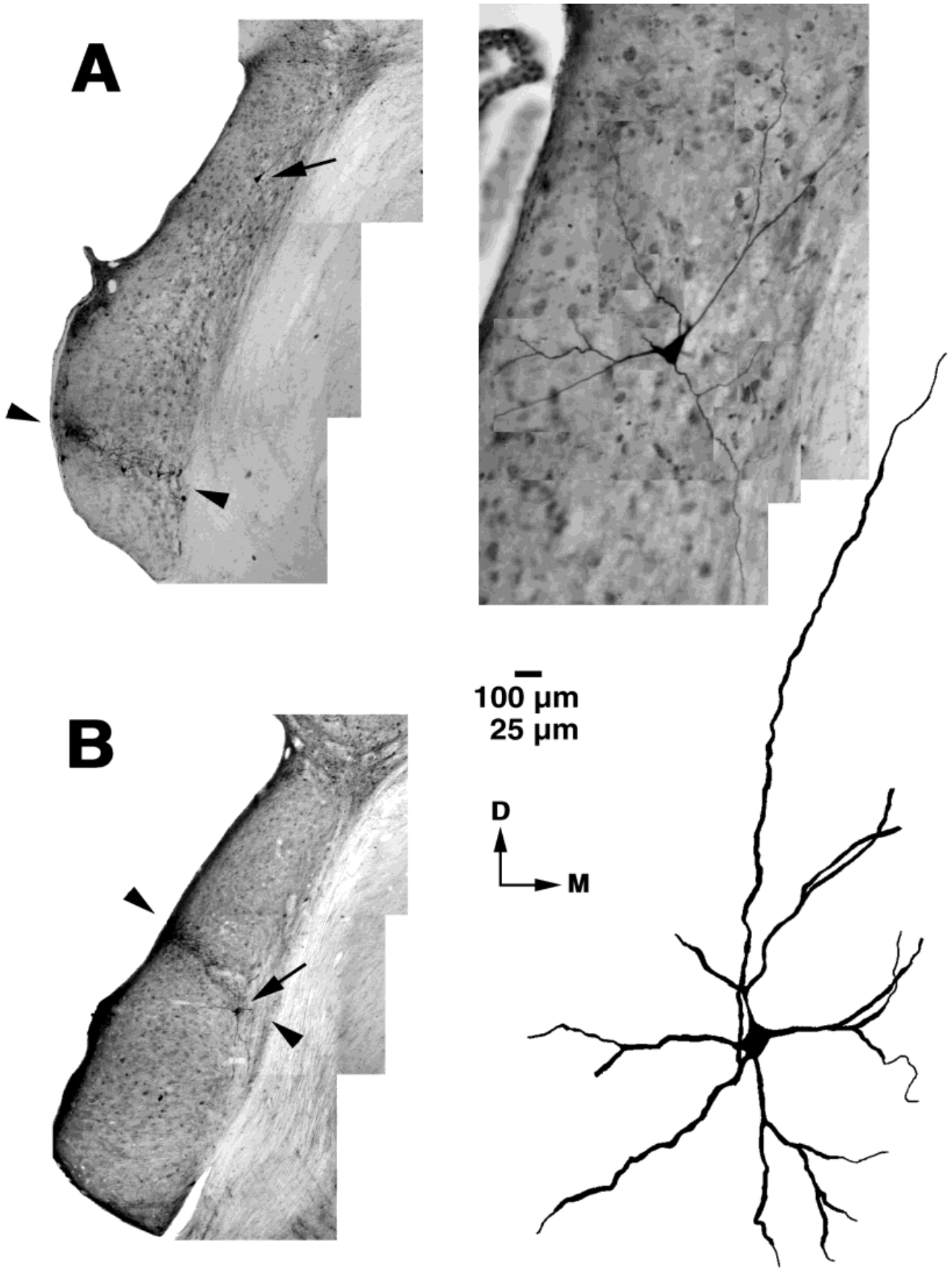

Figure 3

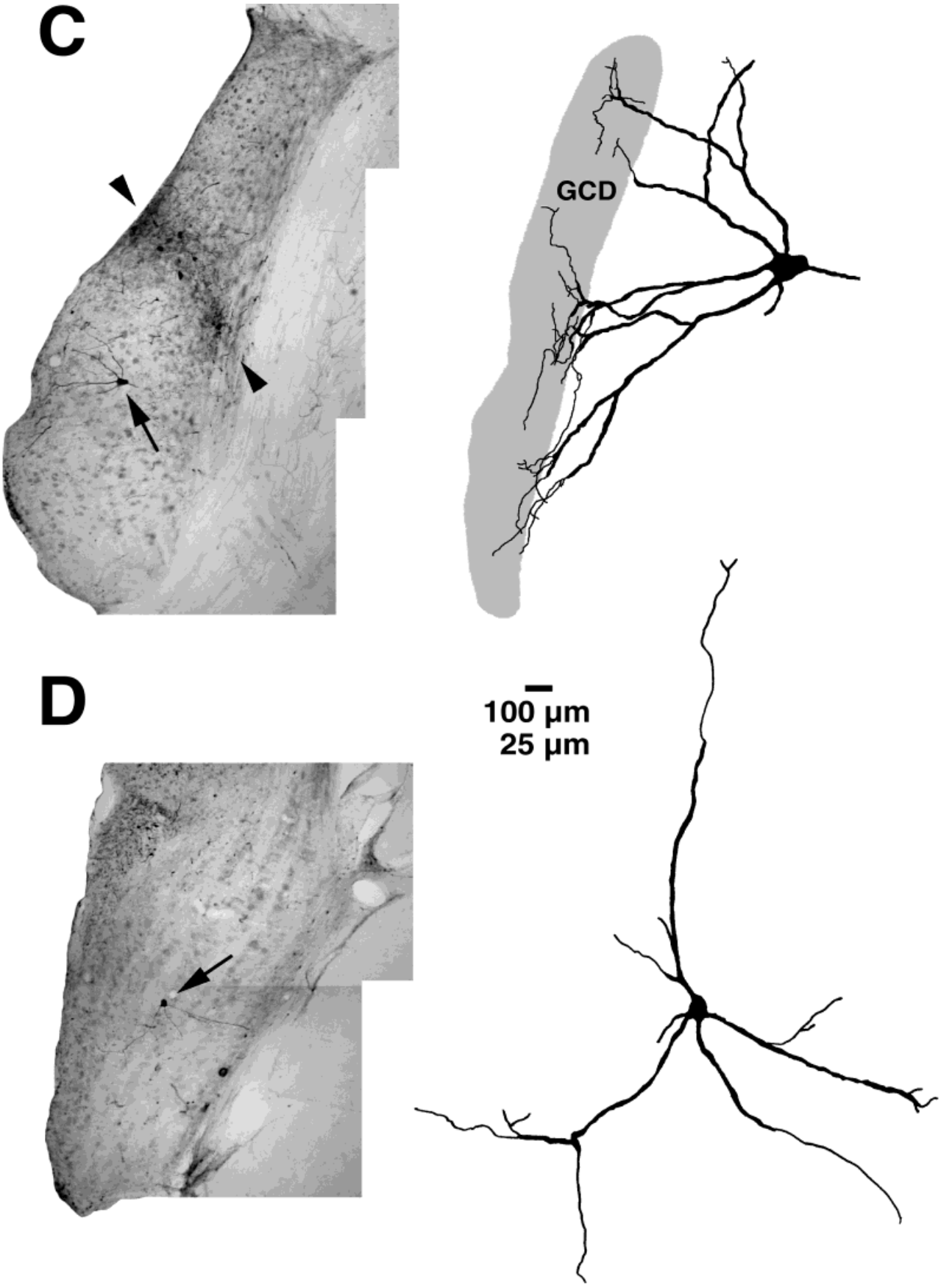

Figure 3 (Continued.)

ments, every section through the cochlear nucleus was drawn with the aid of a light microscope and a drawing tube (total magnification, ×125). The position of each labeled cell was mapped in its proper place onto the appropriate section using blood vessels and tissue borders as landmarks. Verification of labeled and unlabeled cells was conducted at higher magnification (total magnification, ×312) where each section of the VCN was systematically examined.

In order to study structural features of the labeled cells in greater detail, high magnification drawings of labeled cell bodies were performed at a total magnification of ×2500 (100× oil immersion objective, NA = 1.25). The cell body outlines were digitized and their areas determined using NIH Image software (version 1.60). Values are presented as means ± standard deviations, and comparisons between different cell populations were made using Student's two-tailed *t*-test.

The dendrites of labeled cells were reconstructed through adjacent serial sections (40× oil objective, NA = 1.0) in order to assess the orientation and branching patterns of the neurons. Reconstructions were accomplished by aligning the cut ends of dendrites from the surface of one section to the facing surface of the adjacent section. Our criterion required that at least two dendritic branches match in the adjacent section in order that they be drawn; thus, we have probably underestimated the dendritic extent of the labeled cells.

Photographs of all sections and single cells were captured using a 35 mm SLR camera, or a chilled CCD color camera (Hamamatsu) connected to a Macintosh computer. Images were digitized, adjusted (if necessary) using methods consistent with standard darkroom techniques (Adobe Photoshop), and printed in high resolution format (Fuji Pictrography 3000).

RESULTS

General observations

Microneurons of the granule cell domain. Certain aspects of the retrograde labeling observed in the VCN after BDA-injections into the DCN were independent of the injection site. Numerous small cells were labeled and distributed throughout the granule cell domain (Fig. 1A). Due to our interest in the VCN, we examined the superficial layer of granule cells lying along the lateral surface of the VCN, the subpeduncular corner of granule cells sandwiched between the dorsal boundary of the VCN, and the inferior cerebellar peduncle, and the lamina of granule cells separating VCN from DCN. Many of the labeled cells were readily identifiable as granule cells (Fig. 1B). These cells exhibit characteristically smooth, round-to-oval somata of 6–8 μm in diameter, and give rise to two to four primary dendrites of varying lengths and branching frequency. Each dendritic branch ends in a distinctive claw-like structure, but the claw can vary in form from a relatively simple three-pronged spur to a complex arborization. These cells are distributed in the granule cell domain throughout the rostral-to-caudal extent of the cochlear nucleus (Mugnaini et al., 1980b; Weedman et al., 1996).

A second cell type which was least commonly labeled after an injection into the superficial layers of the DCN is the unipolar brush cell (Fig. 1C). The labeled UBC, whose cell body is similar in size to that of granule cells, is nevertheless distinguishable in the light microscope by virtue of its single thick (3–6 μm in diameter) dendrite which erupts after a short distance into a dense spray of fine (<1 μm in diameter) processes (Floris et al., 1994; Wright et al., 1996). This dendritic spray varies in density and can resemble a spiral whorl that enfolds a central space occupied by a single mossy fiber ending (Weedman et al., 1996).

The chestnut cell (Weedman et al., 1996) is the third type of retrogradely-labeled neuron observed in the granule cell domain (Fig. 1D). This cell type was also less commonly labeled by DCN injections than granule cells but more frequently encountered than unipolar brush cells. The most striking light microscopic feature of the chestnut cell is its unusually irregular somatic perimeter and the absence of any clearly definable dendrites. One or two short, stubby appendages can emerge directly from one side of the small (~10 μm) soma, but there is no dendritic stalk as seen in the unipolar brush cell. Fine fingerlike projections emanate from the dendrite-like appendages and the cell body.

These three cell types of the granule cell domain were always found after injections of BDA in the DCN. Labeled microneurons outnumbered labeled neurons in the magnocellular core of the VCN. The ratio of labeled microneurons to labeled macroneurons ranged from roughly 2:1 to greater than 10:1 but averaged around 5:1. Low ratios were correlated with more medial injections in the DCN and higher ratios with more lateral injections. The distribution of labeled microneurons was plotted but it was uncertain whether there was a systematic relationship to the location of the injection site. It appeared that lateral injections in the DCN produced labeled cells in more anterior regions of the VCN, whereas medial injections labeled cells more posteriorly. There was considerable spatial overlap in these distributions, and much more work is needed to clarify this issue. Whether individual cell types in the granule cell domain preferentially innervate different regions of the DCN, and whether there are additional as yet still unidentified cell types within the granule cell domain are additional questions that remain to be determined.

The magnocellular VCN. The main focus of this report is on the pattern of labeling observed in the magnocellular region of the VCN where the neurons with ascending axonal projections reside. When retrograde labeling was observed in any given section, its most obvious feature was a thin band of label distributed across the medial-to-lateral extent of the nucleus (Fig. 1A). The thickness of the band and the number of retrogradely-labeled neurons were directly related to the size of the injection site in the DCN. Bands were composed of labeled cell bodies, dendrites, and numerous segments of labeled axons and terminal swellings (Fig. 2). The source of these axons and terminal swellings probably include anterogradely-filled DCN vertical cells that project tonotopically to the VCN (Wickesberg and Oertel, 1988; Zhang and Oertel, 1993b), retrogradely-filled auditory nerve fibers that project tonotopically throughout the nucleus (Ryugo and May, 1993), and perhaps even collaterals of retrogradely-labeled VCN neurons (Lorente de Nó, 1981; Friauf and Ostwald, 1988). We frequently observed labeled axons in the auditory nerve root, verifying that a subset of the terminals derive from auditory nerve fibers.

The labeled terminal swellings are important in interpreting how the topography of the VCN-DCN projection interacts with the tonotopic organization of the AVCN and

PVCN. We determined that roughly 80% of the labeled somata were coextensive with the VCN region defined by these terminal swellings. Thus, the majority of VCN stellate neurons that project to the DCN receive input from the same auditory nerve fibers that innervate the DCN injection site. The remaining 20% of the labeled cells could lie above or below the band of labeled fibers, sometimes hugging the borders around the granule cell domain, the octopus cell region posteriorly, or the vestibular nerve root medially. Labeled cells were found in both the PVCN and AVCN with the exception of the octopus cell region in the PVCN and the anterior pole of the AVCN, both of which were distinctly lacking labeled cells.

Within the magnocellular region of the VCN, many neurons were found where the BDA reaction product had filled the cell dendrites to allow sufficient characterization. Without any exceptions, every such neuron was of the stellate cell class. That is, each labeled cell body gave rise to two to six primary dendrites. These dendrites projected away with a rather straight trajectory and branched at relatively regular intervals. We never observed dendritic profiles characteristic of bushy cells (globular or spherical) where secondary and tertiary dendritic branch points occurred in a cluster, or of octopus cells where dendrites, resembling trailing tentacles, were distributed in a narrow cone along one side of the cell body.

Multipolar neurons that project to the DCN

Multipolar neurons, so called because of the shape of their cell body, also known as stellate cells when their dendrites are visible, are found throughout the rostral-to-caudal length of the VCN. This class of neuron has historically included a motley assortment of different types (Osen, 1969; Brawer et al., 1974; Lorente de Nó, 1981) that are only recently beginning to be more fully described (Cant, 1981; Cant and Gaston, 1982; Smith and Rhode, 1989; Hackney et al., 1990; Oertel et al., 1990; Benson et al., 1996; Schofield and Cant, 1996). On the basis of cell body size, dendritic orientation, and proximity to the band of labeled cells and fibers, the retrogradely-labeled multipolar neurons lying within the magnocellular core region of the AVCN and PVCN can be divided into at least two separate groups. The first group was distinguished easily from other labeled neurons because of the unusually large size of their cell bodies (diameter, 22–26 μm; mean somatic silhouette area, 466.6 ± 137.1 μm^2) and the thick dendrites that radiated widely across much of the nucleus (Fig. 3). Because of this striking dendritic feature, these neurons are called *radiate cells.* Note that the dorsal-to-ventral orientation of the dendrites of radiate cells is perpendicular to the isofrequency sheets formed by bands of auditory nerve fibers, suggesting that radiate cells receive input from wide regions of the cochlea. Radiate cells were found in both the AVCN (Fig. 3A–C) and PVCN (Fig. 3D). Their somata could be found above (Fig. 3A), within (Fig. 3B), or below (Fig. 3C) the sheet of labeled cells and fibers. For any single case, we observed radiate neurons to be distributed throughout the nucleus without any particular relationship to the labeled sheet. Thus, the dendrites of the population of radiate cells labeled in each experiment could collectively span the entire dorsal-to-ventral axis of the VCN.

A distinguishing feature of the dendrites of radiate neurons is that their distal tips frequently extend into the granule cell domain of the cochlear nucleus (Fig. 3C). Depending on somatic location, dendritic processes were extended into the nearest and most proximal region of the surrounding granule cell domain. Caudally-distributed cells projected their dendrites into the lamina between the PVCN and the DCN, laterally located cells extended into the superficial layer of granule cells along the lateral edge of the AVCN, dorsally-located cells reached the subpeduncular region in the dorsomedial part of VCN, and medially positioned cells contacted the medial sheet of granule cells or sometimes even intermingled with fibers associated with the vestibular nerve root.

The second group of multipolar neurons were distributed within the band of retrogradely-labeled fibers. These cells were significantly smaller than radiate neurons (mean somatic silhouette area, 249.9 ± 95.6 μm^2; $P < 0.0001$), having diameters between 16 and 20 μm. Individual cells and their dendrites within the band were usually so intermixed with labeled fibers and processes from other cells that few could be reconstructed in their entirety. In a few instances, however, neurons were sufficiently separated from their neighbors to allow reconstruction (Fig. 4). The dendrites of these neurons run in a medial-to-lateral direction and are confined to a plane defined by the band of retrogradely-labeled cells and fibers. Because of the orientation of their dendrites, we named these neurons *planar cells.* Although our sample of reconstructed planar cells is small, we infer that these examples are typical since the bulk of the processes within a band have a similar medial-to-lateral orientation and no processes (excluding radiate neuron dendrites) stray from the band. Although no single planar cell extended its dendrites across the entire nucleus, the population of planar cells from each animal collectively spanned the entire medial-to-lateral extent of the VCN.

Surrounding the magnocellular core of the VCN but bounded dorsally and laterally by the granule cell domain and medially by fiber tracts, lies a region of the nucleus populated by small multipolar cells (Osen, 1969; Brawer et al., 1974; Cant and Morest, 1979; Hackney et al., 1990). In this region, we observed retrogradely-labeled multipolar neurons that were distinct from both the planar and radiate cell classes described above. Because these cells were distributed around the periphery of the magnocellular core, we named them *marginal cells.* Marginal cells were found at the ends of the band of labeling in a given coronal section, and they were observed far outside the band (Fig. 5A). Typically, these cells have one or two prominent dendrites oriented parallel to the boundary of the granule cell domain or medial border of the VCN, and as a result, these dendrites help define the border between granule cell domain and the magnocellular core. At least one dendrite also projects into the core region of the VCN. In spite of some common features with radiate cells,

Fig. 4. Photomicrograph (**A**) and drawing tube reconstructions of typical BDA-labeled planar neurons (**B–D**). The cell bodies of planar neurons are found in the band of labeling and their dendrites are confined to this band. Note that this orientation is parallel to the path of incoming auditory nerve fibers. In (A) a photomicrograph of a coronal section through the PVCN is shown containing the cell body (denoted by arrow) of the planar neuron reconstructed in B. C, D: Two reconstructed planar neurons whose cell bodies were located in the AVCN. There was no apparent difference between planar neurons of the AVCN and PVCN. The scale bar refers to all panels. D, dorsal; M, medial.

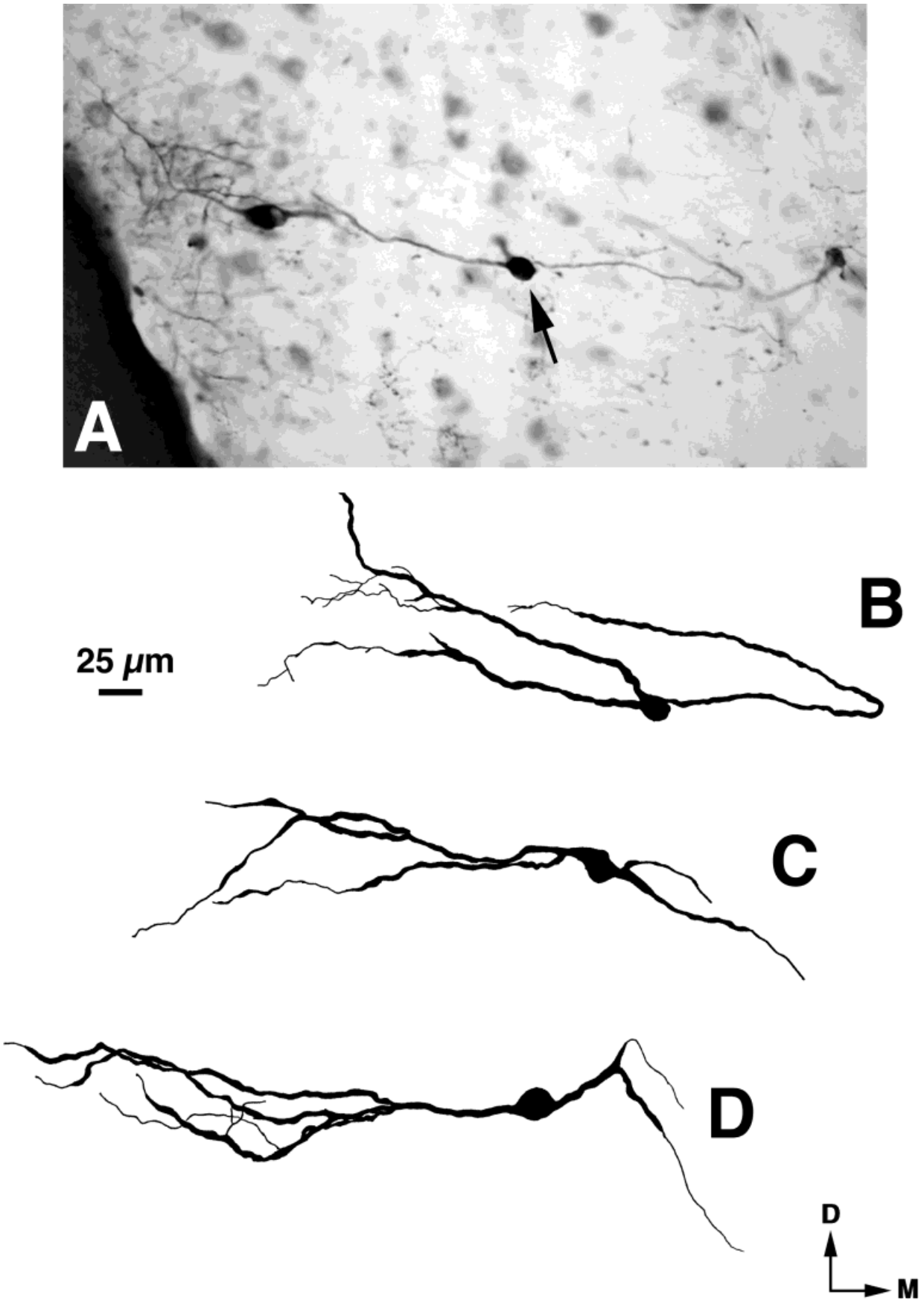

Figure 4

marginal cells were not grouped with radiate neurons because of their smaller cell body size (mean somatic silhouette area, 230.3 ± 87.2 μm^2) and because their dendrites span a much more restricted region (50–100 μm for marginal cells vs. 250–350 μm for radiate cells). Some labeled cells found along the margins did not readily fit into any category, but they were so infrequent that they were not considered further.

Topography of VCN projections

In those cases where tissue was counterstained with cresyl violet, labeled cells could be examined in the context of their cytoarchitectonic nuclear subdivision using criteria previously defined (Ryugo et al., 1981; Hackney et al., 1990). As we have already mentioned, the position of microneurons within the granule cell domain did not have any clear relationship to the DCN injection site. For this reason, we focused on the topography of the labeled multipolar neurons in the magnocellular regions of the VCN. Since every labeled cell and its dendrites could not be reconstructed, we applied the following method for identifying labeled cells. Radiate neurons were identified by virtue of their large size and long, radiating dendrites. Marginal cells were non-radiate labeled cells that were located more than 100 μm from the subjective center of the band of labeling. Neurons within the band of labeled fibers were identified as planar cells, except for cells near the lateral and medial boundaries of the band that could unequivocally be identified as marginal cells (because of the dorsoventral orientation of their dendrites). The positions of labeled cells are plotted using three symbols representing the three classes of multipolar cells that have been described.

Injections confined to the medial aspect of the DCN (n = 4) produced a band of labeled planar cells distributed across the medial-to-lateral width within the dorsal region of the VCN (Fig. 6). Radiate neurons are lightly scattered either within or outside the band and marginal cells are distributed along the boundaries of the VCN. Unlike radiate neurons that were distributed throughout the dorsal-to-ventral axis of the VCN, we rarely observed labeled marginal cells ventral to the band. The caudal distribution of labeled planar and radiate neurons does not reach the posterior pole of the PVCN but originates immediately anterior to the octopus cell region. The band of labeled planar cells in each coronal section, when combined with bands of the other coronal sections, forms a three-dimensional sheet that extends smoothly towards, but does not reach, the anterior pole of the AVCN. Injections in the middle regions of the DCN (n = 3) produced a sheet of labeled planar cells situated in the middle regions of the VCN (Fig. 7), whereas ventrolateral injection sites (n = 3) produced labeled planar cells distributed more ventrally (Fig. 8).

In addition to the dorsoventral topography of the labeled sheets of neurons, there was also an anterior-posterior topography. Injections in the ventrolateral DCN resulted in a caudal distribution of labeled neurons that extended beneath the overlying octopus cell region and reached the posterior boundary of the PVCN. The anterior distribution of labeled neurons passed through the auditory nerve root region (interstitial nucleus of Lorente de Nó, 1981) but did not reach the anterior pole of the AVCN (Fig. 8). Injections in progressively more medial regions of the DCN produced sheets of labeled cells that began anterior to the octopus cell region and extended progressively more rostrally (Figs. 6, 7). There was no apparent anterior-posterior topography related to the distribution of radiate or marginal cells with respect to DCN injection sites.

Both the VCN and the DCN are organized tonotopically. In the VCN, high CF auditory nerve fibers terminate dorsally while lower CF neurons innervate successively more ventral regions of the VCN. In the DCN, high CF neurons terminate medially while low CF neurons project to more lateral regions of the DCN. In Figures 6–8, we demonstrated that as the injection site moved from medial to lateral positions within the DCN, we observed that the band of labeled fibers and planar cells moved from dorsal to ventral positions within the VCN. This result implies that like the cat cochlear nucleus (Snyder and Leake, 1988), the majority of the connections between the core regions of the VCN and the DCN are between corresponding isofrequency sheets.

DISCUSSION

The results of the present study reveal that microneurons of the granule cell domain and multipolar macroneurons of the VCN both project to the DCN. The microneurons include granule cells, unipolar brush cells, and chestnut cells. In addition, a small population of small-to-medium sized multipolar cells project to the DCN and these neurons, called marginal cells, are found immediately internal to the granule cell domain along the borders of the VCN. It could not be unambiguously determined if these cell populations are preferentially and/or topographically related to injection sites in the DCN. The organization of the macroneuronal projections are summarized in Figure 9. Planar neurons have dendrites that lie within an isofrequency lamina and project to the corresponding isofrequency lamina in the DCN. Radiate neurons have dendrites that extend across isofrequency laminae in the VCN and they very likely innervate broad frequency regions in the DCN. Our results do not directly demonstrate the broad terminal field for the radiate neuron, but we did observe considerable overlap between the frequency regions of the VCN containing labeled radiate neurons after each injection site. In support of our interpretation, a VCN multipolar cell type in mice, named the D-stellate neuron, is analogous in many ways to radiate neurons (discussed below) and has been shown to have a broad terminal field in the DCN (Oertel et al., 1990).

When defining the pattern of neuronal connections using extracellular dye injections, it is always necessary to consider the possibility of nonspecific labeling caused by dye uptake through severed axons of passage or leakage

Fig. 5. Photomicrograph (A) and drawing tube reconstructions of typical BDA-labeled marginal cells (B–F). **A:** This photomicrograph of a coronal section through the PVCN shows the location of the reconstructed marginal cells in **B–D**. In this experiment, the BDA-injection was centered in the ventrolateral DCN. The marginal cells in **E** and **F** were taken from two different experiments and were located in the AVCN. Marginal cells are so named because their cell bodies are located along the margins of the VCN, and they typically have one or two dendrites that run along the borders of the magnocellular core region of the VCN, usually near the boundaries of the granule cell domain. An additional dendrite usually projects into the magnocellular core. Marginal cells of the AVCN and PVCN very much resemble each other structurally. D, dorsal; M, medial.

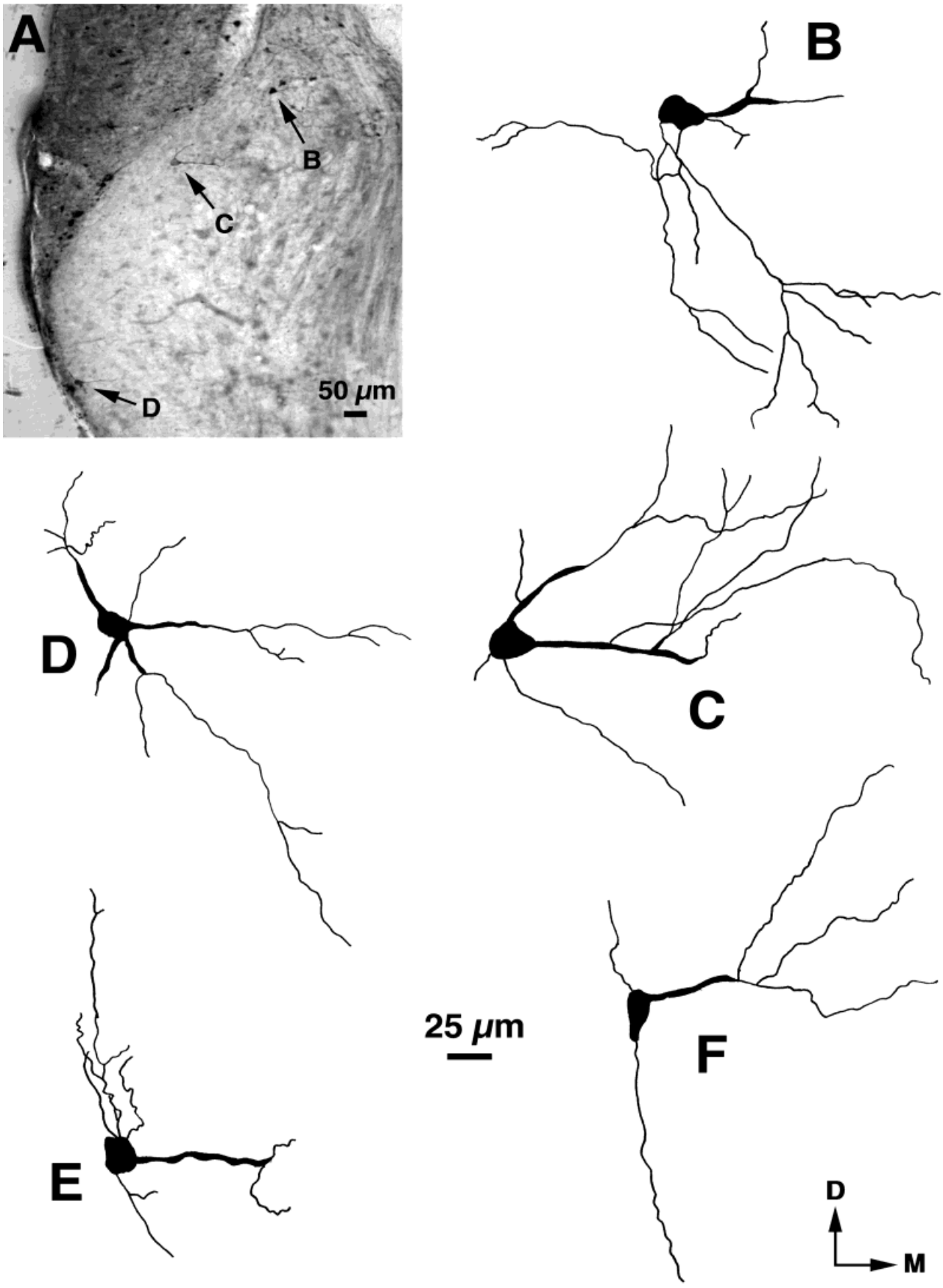

Figure 5

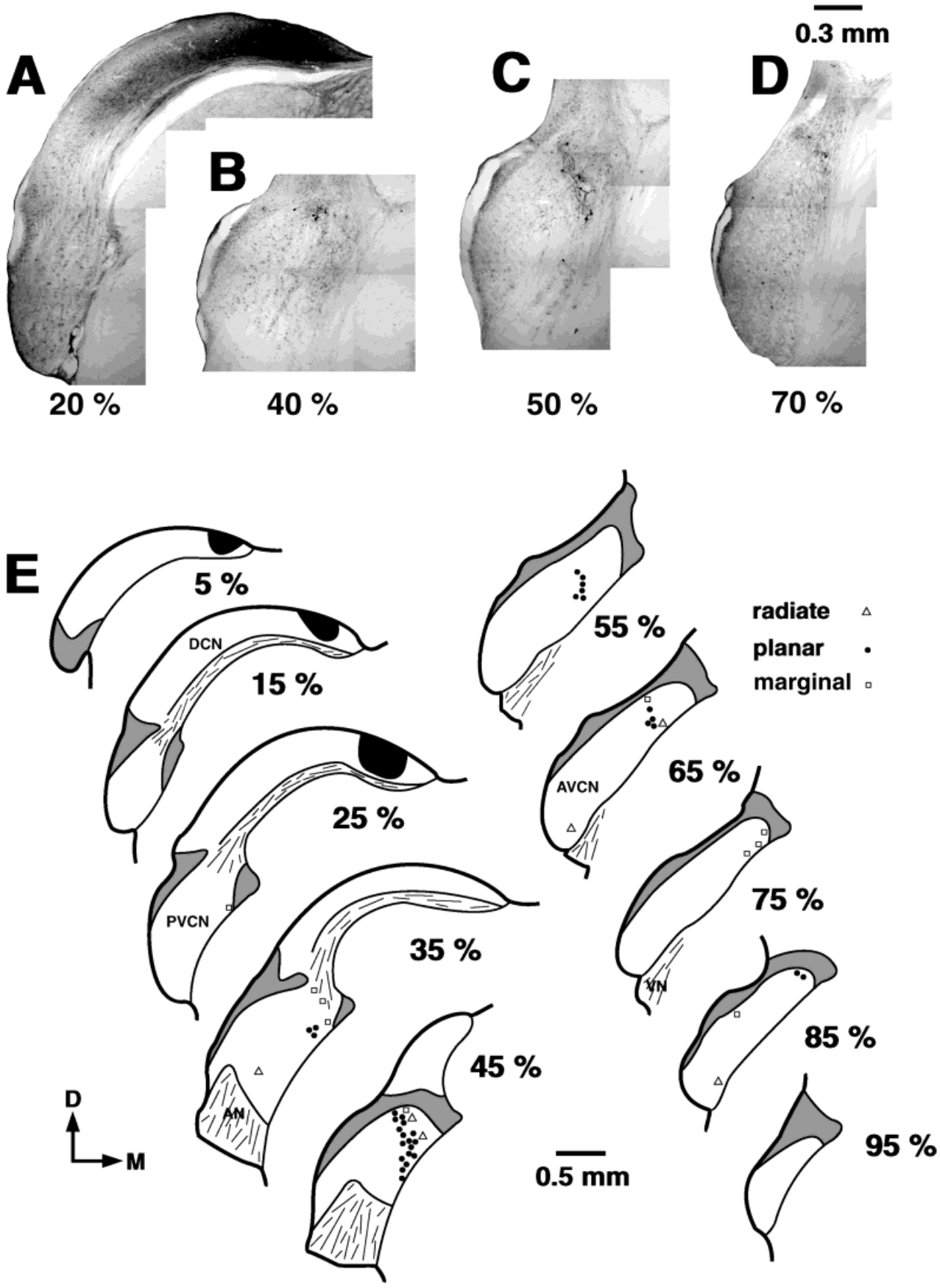
A
B
C
D
0.3 mm
20 %
40 %
50 %
70 %
E
5 %
DCN
15 %
25 %
PVCN
35 %
45 %
AN
55 %
AVCN
65 %
75 %
VN
85 %
95 %
radiate
planar
marginal
D
M
0.5 mm

Figure 6

into other sites. Since some VCN multipolar neurons project their major axons dorsally (Friauf and Ostwald, 1988, Smith and Rhode, 1989; Oertel et al., 1990), extracellular dye injections must be confined within the DCN in order to interpret accurately the subsequent retrograde labeling found in the VCN. All data presented in this manuscript are derived from animals in which the injection site was histologically confirmed to be located within the DCN; no extracellular reaction product was found elsewhere. The absence of labeled pyramidal and giant cells outside the injection site and the absence of labeled octopus cells in the VCN indicate that our injections did not leak into the dorsal or intermediate acoustic striae which travel just ventral to the DCN, because these cell types send their axons through these striae. On the other hand, the path of the injection pipette through the DCN molecular layer severed and probably labeled some parallel fibers passing through the injection site, and this contamination might have obscured any topographic relationship that exists between microneurons in the granule cell domain and the DCN.

We have demonstrated that the dorsomedial to ventrolateral extent of the DCN receives a robust innervation from multipolar neurons of the VCN. This projection can be partitioned into two "streams" of unequal magnitude. The first stream is conducted by planar neurons that represent 80–90% of the projecting neurons. Planar neurons are characterized by dendrites that restrict themselves to more-or-less horizontal sheets, where collectively they coincide with the paths and arborizations of incoming auditory nerve fibers. This sheet-like organization reflects what has been called fibrodendritic layering (Ramón y Cajal, 1909; Poljak, 1926) and most likely represents the cellular foundation for the tonotopic organization of the nucleus (Bourk et al., 1981; Ryugo, 1992). The intermingling of labeled planar neurons and auditory nerve fibers suggests that planar neurons are innervated by the same auditory nerve fibers that terminate within the DCN injection site.

The second stream is conveyed by radiate and marginal neurons, the remaining 10–20% of the projection. Marginal neurons are characterized by their thin dendrites that either run parallel to the borders of the nucleus or project into the core of the VCN. The distribution of marginal cells depended on the DCN injection site; they were almost always located dorsal to the band of planar cells labeled by a given DCN injection. Radiate neurons are characterized by long dendrites that extend over great distances and in all directions, traversing broad frequency regions of the VCN. Independent of the DCN injection site, radiate neurons could be found at any position along the dorsal-ventral axis of the VCN and as a result, they exhibit a nontonotopic projection to the DCN. The population of radiate neurons labeled in any given experiment usually spanned the entire frequency domain of the VCN. The dendritic orientation and pattern of projections of marginal and radiate neurons suggests that auditory nerve activity, regardless of its cochlear origin, can influence broad regions of the DCN through the actions of these multipolar neurons.

Microneurons of the granule cell domain

The number of labeled microneurons of the granule cell domain after a DCN injection was roughly five times that of labeled macroneurons of the VCN. There appeared to be a very crude topography to this projection, where microneurons of the anterior granule cell domain projected to the low frequency regions of the DCN and progressively more posteriorly-located microneurons projected to progressively higher frequency regions. This pattern resembles the rough cochleotopic projection exhibited by Type II spiral ganglion cells (Brown et al., 1988a; Brown and Ledwith, 1990; Berglund and Brown, 1994). The axons of cochlear granule cells are known to synapse on the apical dendrites of cartwheel, pyramidal, and stellate cells (Mugnaini et al., 1980a,b; Wouterlood et al., 1984; Berrebi and Mugnaini, 1991; Ryugo et al., 1995). By virtue of sheer numbers alone, cells of the granule cell domain produce the bulk of the *ventrotubercular projections* and must have an important role in neural processing. This role, however, may not be the direct processing of rapidly-conducted cochlear input because the granule cell domain receives few terminals from myelinated auditory nerve fibers (Osen, 1970; Fekete et al., 1984). The granule cell domain is the recipient of significant descending projections from higher auditory structures, including medial olivocochlear neurons (Brown et al., 1988b), the inferior colliculus (Caicedo and Herbert, 1993; Malmierca et al., 1996), and auditory cortex (Feliciano et al., 1995; Weedman and Ryugo, 1996a,b). It is also the target of inputs from somatosensory structures (Itoh et al., 1987; Weinberg and Rustioni, 1987; Wright and Ryugo, 1996) and the vestibular end organ (Burian and Goesttner, 1988; Kevetter and Perachio, 1989). The granule cell domain is well situated to influence the output of the DCN, and it may be involved in the integration of body, head, and pinna position with acoustic information for locating sounds while the animal is moving (Young et al., 1995; Wright and Ryugo, 1996).

Within the granule cell domain, a circuit diagram that describes the mechanisms of signal transfer via specific cell types is not yet possible because so little is known about the synaptic organization, axonal trajectories, and postsynaptic targets of these microneurons. Granule cells, unipolar brush cells, and chestnut cells receive mossy fiber endings, but only a small portion of such endings have been traced to their origin (Wright and Ryugo, 1996). What contacts the distal tips of radiate cell dendrites in the granule cell domain also remains to be determined. Within the granule cell domain, there is a surprising number of

Fig. 6. Distribution of BDA-labeled cells in the VCN from a single experiment where the injection was centered in the medial (high frequency) region of the DCN. A–D are photomontages of coronal sections through the cochlear nucleus with normalized position (in percentile) of each section along the rostrocaudal axis of the nucleus. **A:** This montage confirms that the injection site is confined to the dorsomedial region of the DCN. **B–D:** These montages display the characteristic band of labeled cells and processes found throughout the VCN. Note that the band is located near the dorsal border (high frequency region) of the VCN. **E:** Coronal atlas of the cochlear nucleus at 10% intervals illustrating the position of labeled cells in the VCN. Each symbol represents the location of a single labeled cell body, and three different symbols are used to represent planar, radiate, and marginal cells. The position of planar neurons is restricted to the band of retrograde labeling seen in B–D. In contrast, radiate neurons are sprinkled all along the dorsoventral axis of the VCN. Marginal cells hug the lateral, dorsal, and medial borders of the magnocellular core of the VCN. Notice the absence of labeled cells in the caudal PVCN (octopus cell area) and the rostral AVCN (spherical cell area). AN, auditory nerve; AVCN, anteroventral cochlear nucleus; D, dorsal; DCN, dorsal cochlear nucleus; M, medial; PVCN, posteroventral cochlear nucleus; VN, vestibular nerve.

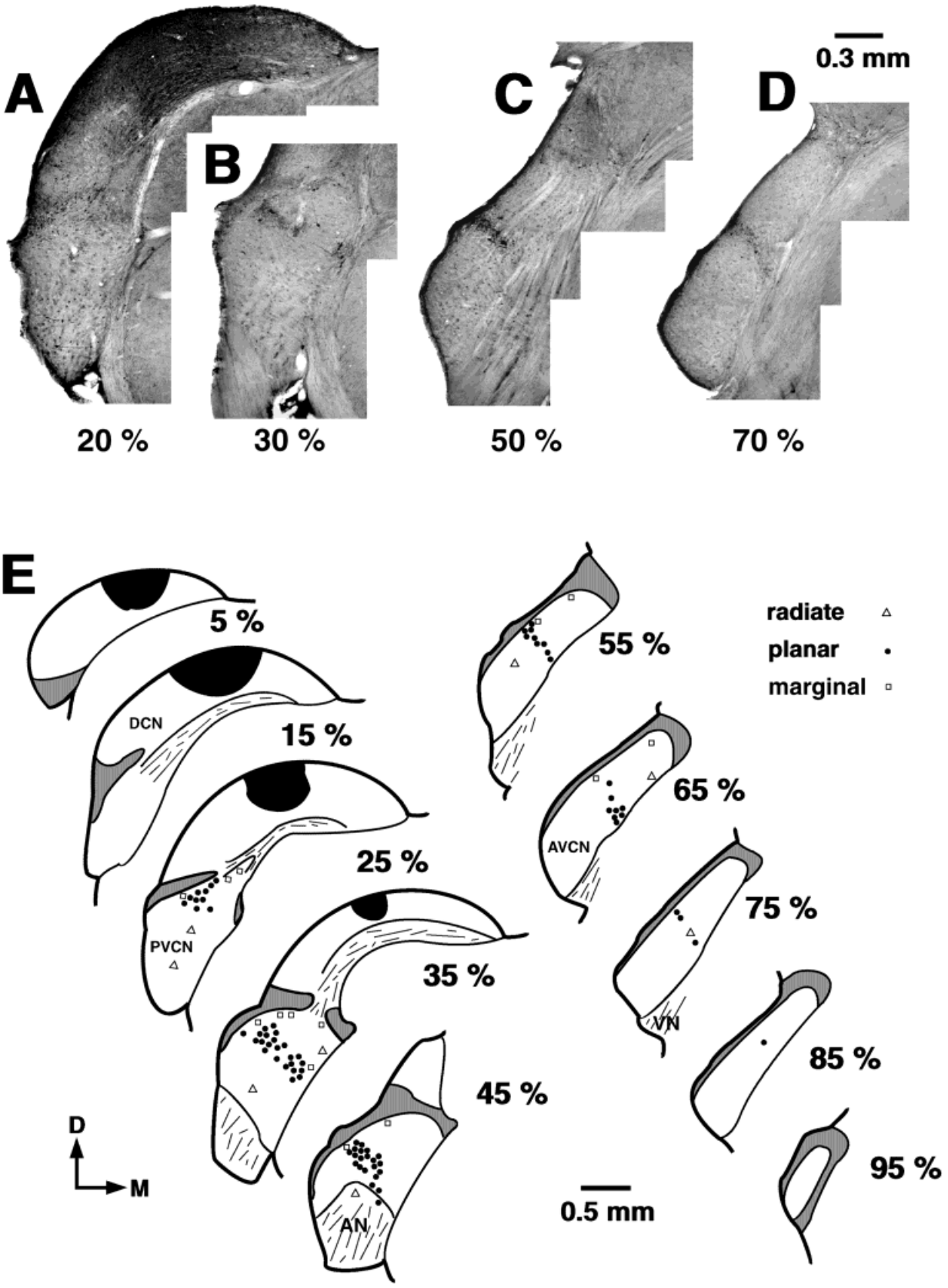

Fig. 7. Distribution of BDA-labeled cells in the VCN from an injection centered in the middle (mid-frequency region) of the DCN. **A:** This montage indicates the injection site and corresponding bands of labeling in the VCN are seen in **B–D**. The labeled cells are located midway along the dorsoventral axis (mid-frequency region) of the VCN. **E:** Coronal atlas of the cochlear nucleus with locations of labeled cells. Note that the sheet of labeled cells in the middle region of the VCN has shifted caudally compared to the sheet located in the dorsal region of the VCN (Fig. 6E). A detailed description of the format, symbols, and abbreviations can be found in the legend for Figure 6.

labeled, small caliber fibers and swellings. Although we observed only short segments of the labeled fibers, they had the "lumpy" appearance of group VI axons stained by the Golgi method in the granule cell domain of kittens (Cant and Morest, 1978). Presumably these fibers belong to the retrogradely labeled microneurons, and they could be synaptically interacting with other microneurons of the granule cell domain. It is also possible that some of these labeled fibers and swellings represent a previously undescribed projection from the DCN or that they are collaterals of the ventrotubercular projection. What is certain is that there is still much to be learned about the granule cell domain.

Multipolar neurons of the VCN: Functional implications

Multipolar cells, also known as stellate cells, are ubiquitous throughout the VCN. Clear differences between multipolar neurons have been demonstrated by a number of authors using different species and different criteria. Observations in rodents, guinea pigs, and cats have made distinctions between multipolar cells on the basis of cell body size (Osen, 1969), ultrastructural features (Cant, 1981), ascending projections (Cant, 1982), single cell recording and staining (Smith and Rhode, 1989; Oertel et al., 1990), and dendritic morphology (Lorente de Nó, 1981; Hackney et al., 1990). To what extent categories are similar or different between the AVCN and PVCN still remain to be determined. On the one hand, it is possible that these groupings represent the true diversity of multipolar cell types in the VCN. On the other hand, it is also possible that these different classification criteria refer to the same neuron classes. The organization of these neurons with respect to their connections and physiological properties will be key to understanding the cellular mechanisms of how the cochlear nucleus processes acoustic information.

Marginal neurons

Marginal neurons in the rat reside in a region of the VCN that resembles the small cell cap in cats (Osen, 1969) and guinea pigs (Hackney et al., 1990). The small cell cap forms a shell around the magnocellular core of the VCN, bordered laterally and dorsally by the granule cell domain and medially by the vestibular nerve root and trapezoid body fibers. Neurons within this peripheral region exhibit dendrites that, unlike most multipolar neurons within the core of the VCN, were oriented in a dorsal-to-ventral direction and thus perpendicular to the orientation of isofrequency sheets (Osen, 1969; Brawer et al., 1974; Cant and Morest, 1979). We have also observed this dendritic orientation, and have now shown that at least a portion of these small multipolar neurons ringing the core of the VCN project their axons to the DCN.

Recent studies have begun to provide insight to the inputs and physiology of cells in the small cell cap. The small cell cap is almost exclusively innervated by low and medium spontaneous rate (SR) auditory nerve fibers (Liberman, 1991; Liberman, 1993; Ryugo et al., 1993). Low and medium SR fibers have higher thresholds and wider dynamic ranges than do high SR fibers. Therefore, it is expected that neurons within the small cell cap would be similarly endowed with these properties. Indeed, recordings from neurons near the margins of the VCN reveal that these cells have higher thresholds and wider dynamic ranges in response to tones and noise than do neurons residing within the magnocellular core of the VCN (Ghoshal and Kim, 1996). The wide dynamic ranges in response to tones might also be due to spread of excitation to off-CF neurons, since the dendrites of marginal neurons can intersect the path of auditory nerve fibers having a broad range of CFs.

Hypotheses about the function of marginal neurons and the mechanisms underlying the wide dynamic ranges of neurons near the borders of the VCN will depend on what types of inputs they receive. The dendrites of marginal cells tend to be closely opposed to microneurons of the granule cell domain and some can enter the magnocellular core of the VCN. The bulk of the inputs to the granule cell domain are from *descending* pathways arising from a variety of sources and the inputs to the magnocellular core of the VCN are dominated by *ascending* auditory nerve fibers. If marginal neurons receive inputs from both regions, they become strong candidates for exhibiting the unusual physiological response properties reported near the margins of the VCN (e.g., Bourk, 1976), and they emerge as very interesting players in the integration of neural activity in ascending and descending systems.

Planar neurons

The planar neurons of the rat correspond in many ways to stellate cells classified as sustained chopper units (Chop-S) in cats (Smith and Rhode, 1989) and stellate neurons with axons projecting toward the trapezoid body (T-stellate cells) found in mice (Oertel et al., 1990). Both Chop-S and T-stellate neurons send a collateral towards the DCN in addition to sending their major axon into the trapezoid body. The axonal arborization of one T-stellate cell was distributed in a narrow "isofrequency" band in the DCN (Oertel et al., 1990), and resembles what we predict for planar neurons on the basis of the pattern of their retrograde labeling.

An ultrastructural examination of the cell bodies of intracellularly labeled Chop-S units in the PVCN revealed that they had few primary terminals contacting their cell bodies (Smith and Rhode, 1989). Multipolar cells in the AVCN also exhibiting few somatic terminals were called type I stellate cells (Cant, 1981). These cells project to the contralateral inferior colliculus (Cant, 1982) and send a collateral to the DCN as well (Adams, 1983). Planar neurons project to the DCN, and we observed many labeled fibers in the trapezoid body, indicating that at least some of the labeled multipolar cells project their axons through the trapezoid body. Chop-S units are narrowly tuned, both in terms the shape of their tuning curves to pure tones (Rhode and Smith, 1986) and their inability to integrate acoustic energy when spread over wide frequency bands (Palmer et al., 1996). Chop-S units can be found throughout the VCN (Pfeiffer, 1966; Bourk, 1976; Young et al., 1988). Planar neurons, like T-stellate cells, have dendritic orientations consistent with narrow tuning, being oriented parallel to the path of auditory nerve fibers having similar CFs. Since planar neurons, Chop-S neurons, and multipolar cells with few somatic terminals are all found throughout both the AVCN and PVCN, it is arguable that these all represent the same neuron class.

An isofrequency lamina of the DCN receives two tonotopic projections: an "unprocessed" primary projection from narrowly-tuned auditory nerve fibers and a "processed" projection from similarly-tuned planar neurons.

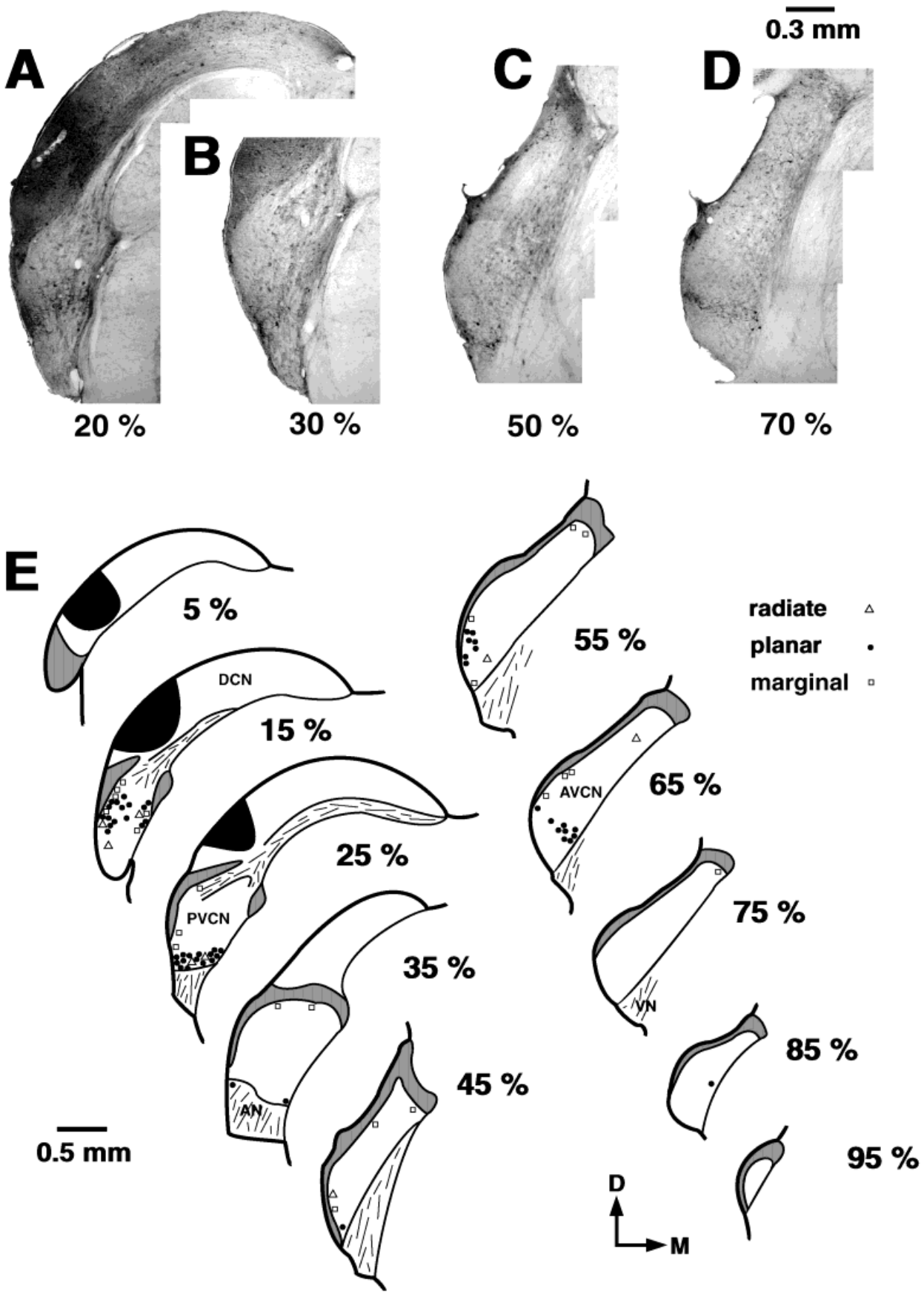
A
B
C
D
0.3 mm
20 %
30 %
50 %
70 %
E
5 %
DCN
15 %
25 %
PVCN
35 %
AN
45 %
55 %
AVCN
65 %
75 %
VN
85 %
95 %
radiate
planar
marginal
0.5 mm
D
M

Figure 8

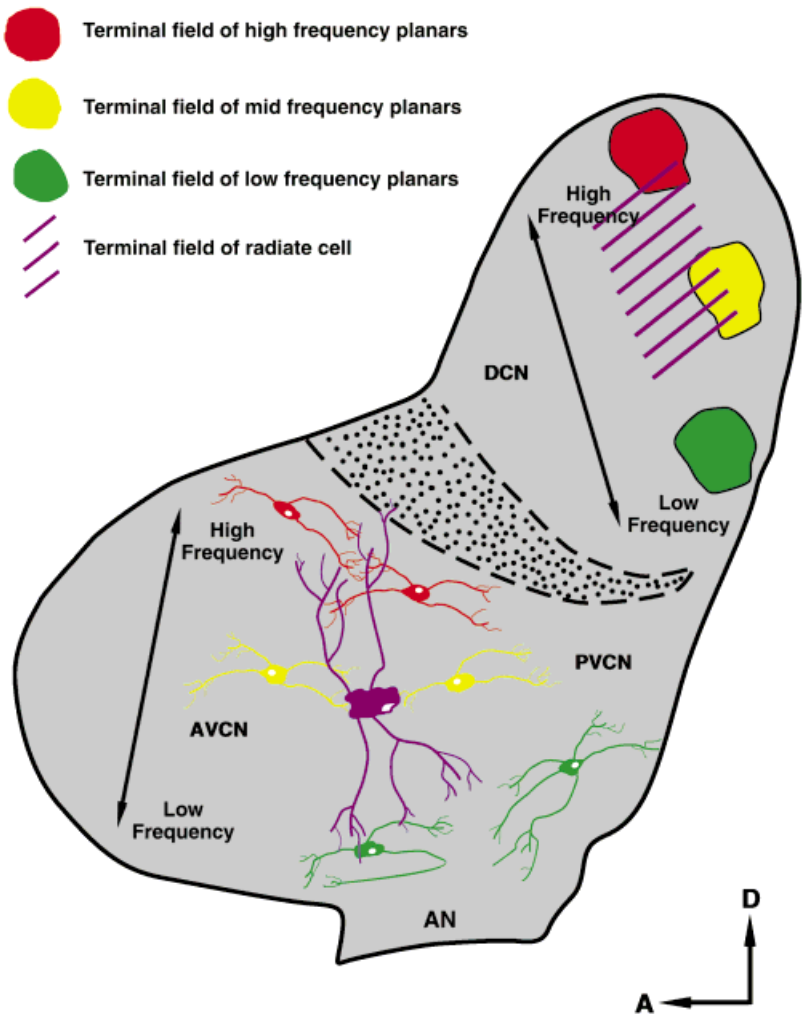

Fig. 9. Schematic diagram summarizing the projections of planar and radiate neurons to the DCN. The frequency axis displayed in both the VCN and DCN is perpendicular to the plane of isofrequency sheets in the two divisions. The stippled region demarcates the granule cell domain. The dendrites of planar neurons are oriented parallel to VCN isofrequency sheets and project to the corresponding isofrequency sheet in the DCN. The dendrites of radiate neurons are oriented perpendicular to the plane of isofrequency sheets and frequently enter the granule cell domain. Unlike planar neurons, radiate neurons likely project to several isofrequency laminae in the DCN. Abbreviations as in the legend for Figure 6.

One unresolved issue is whether planar neurons and auditory nerve fibers contact the same or different cell types in the DCN. Since the terminals of Chop-S neurons contain round synaptic vesicles (Smith and Rhode, 1989), they are presumed to exert excitatory postsynaptic effects. Consistent with this notion is the observation that focal applications of glutamate in the VCN produced excitatory postsynaptic potentials in DCN giant cells when the loci of application conformed to an isofrequency band in the VCN (Zhang and Oertel, 1993a). Which other DCN cell types are contacted by Chop-S neurons is unknown, but a single reconstructed T-stellate neuron was shown to terminate near the cell bodies of pyramidal cells (Oertel et al., 1990). These observations are consistent with the idea that planar neurons contact pyramidal and giant cells, cell types that have also been shown to receive auditory nerve fiber input (Gonzalez et al., 1993).

Fig. 8. Distribution of BDA-labeled cells in the VCN from an injection centered in the ventrolateral (low frequency) region of the DCN. **A:** This photomontage illustrates the injection site in the DCN and corresponding bands of labeling in the VCN are shown in panels **B–D**. **E:** Coronal atlas of the cochlear nucleus with locations of labeled cells. This injection yields a band of labeling that is located ventrally (low frequency region) in the VCN. Note also that the sheet of labeled cells passes beneath the octopus cell region and extends to the posterior border of the PVCN. A detailed description of the format, symbols, and abbreviations can be found in the legend for Figure 6.

Radiate neurons

Radiate neurons in the rat share many morphological features with stellate neurons classified as Onset-chopper units (On-C) in the cat (Smith and Rhode, 1989) and to stellate neurons in the mouse that send their major axon dorsally beneath the DCN (D-stellate; Oertel et al., 1990). Both On-C units and D-stellate neurons project a collat-

eral axon into the DCN, but their major axons could not be followed to their termination points outside the cochlear nucleus. Radiate neurons project to the DCN, but at this time it is not known if they also send a major axon elsewhere because the axonal labeling in the dorsal output tracts that we observed could have been due to pyramidal and giant neurons labeled by the DCN injections. The DCN terminal field of one D-stellate neuron was found to extend over a broad region of the DCN (Oertel et al., 1990). Our observation that labeled radiate neurons could be observed in any region of the VCN after a restricted DCN injection is consistent with the idea that single radiate neurons innervate a broad region of the DCN.

Radiate, D-stellate, and On-C units all exhibit relatively large cell bodies and share two atypical dendritic features that tend to unify them as a group. First, the dendrites of these cells are prominent, extending hundreds of micrometers across the path of auditory nerve fibers arising from broad regions of the cochlea. Second, the distal tips of the dendrites frequently penetrate into the granule cell domain. This morphology is also strikingly similar to what has been described for commissural neurons of the VCN (Schofield and Cant, 1996). The radial trajectory of these dendrites is consistent with their being physiologically responsive to a broad range of frequencies, and in fact, On-C units appear to integrate the activity of auditory nerve fibers having a wide range of CFs (Rhode and Smith, 1986; Winter and Palmer, 1995; Jiang et al., 1996; Palmer et al., 1996).

At the ultrastructural level, On-C neurons of the PVCN have cell bodies that are contacted by many terminals (Smith and Rhode, 1989). In the AVCN, the type II stellate cell was identified on the basis of its numerous somatic terminals (Cant, 1981), and while it is not known where these cells project, it is known that they do not project to the contralateral inferior colliculus (Cant, 1982). The terminals of On-C neurons contain pleomorphic synaptic vesicles, indicating that they probably have an inhibitory effect on their target neurons. No direct evidence exists about the types of DCN neurons contacted by On-C neurons, but D-stellate neurons appear to contact giant and vertical cells (Zhang and Oertel, 1993a,b). These observations are consistent with the idea that radiate cells give rise to an inhibitory projection to the DCN.

In order to account for the response properties of type II and type IV units of the DCN, both modeling and physiological studies have proposed that each neuron type is innervated by a broadly-tuned source of inhibition (*modeling studies:* Arle and Kim, 1991; Pont and Damper, 1991; Blum, et al., 1995; *physiological studies:* Winter and Palmer, 1993; Nelken and Young, 1995). For example, Type II neurons are excited by narrowband stimuli within their response areas, but respond weakly or not at all to broadband noise (Young and Brownell, 1976). This property of Type II units could be explained if they receive a broadly-tuned inhibitory input from On-C neurons (Winter and Palmer, 1993). On-C neurons have also been postulated to be the source of wideband inhibition necessary to explain the sensitivity of type IV units to spectral notches (Nelken and Young, 1995). We have shown that each DCN locus is innervated by a complement of radiate neurons whose dendrites collectively span the entire tonotopic axis of the VCN. Because radiate neurons share many of the same cytological features characteristic of On-C neurons, they are strong candidates for being the source of wideband inhibition to the DCN.

ACKNOWLEDGMENTS

We thank Tan Pongstaporn, Brian Rosenbaum, Edward Aboujaoude, and Rachel Urik for technical assistance. We also thank Eric Young, Kevin Davis, and M. Boyd Gillespie for helpful discussions. This work was supported by research grants RO1 DC00232 and P60 DC00979 from the National Institute on Deafness and Other Communication Disorders, National Institutes of Health. Parts of these results were presented in preliminary fashion at the 19th Midwinter Meeting for the Association for Research in Otolaryngology, St. Petersburg Beach, FL, 4–8, February 1996.

LITERATURE CITED

Adams, J.C. (1983) Multipolar cells in the ventral cochlear nucleus project to the dorsal cochlear nucleus and the inferior colliculus. Neurosci. Lett. *37:*205–208.

Arle, J.E., and D.O. Kim (1991) Simulations of cochlear nucleus neural circuitry: Excitatory-inhibitory response-area types I-IV. J. Acoust. Soc. Am. *90:*3106–3121.

Benson, T.E., A.M. Berglund, and M.C. Brown (1996) Synaptic input to cochlear nucleus dendrites that receive medial olivocochlear synapses. J. Comp. Neurol. *365:*27–41.

Berglund, A.M., and M.C. Brown (1994) Central trajectories of type-II spiral ganglion cells from various cochlear regions in mice. Hearing Res. *75:*121–130.

Berrebi, A.S., and E. Mugnaini (1991) Distribution and targets of the cartwheel cell axon in the dorsal cochlear nucleus of the guinea pig. Anat. Embryol. *183:*427–454.

Blum, J.J., M.C. Reed, and J.M. Davies (1995) A computational model for signal processing by the dorsal cochlear nucleus. II. Responses to broadband and notch noise. J. Acoust. Soc. Am. *98:*181–191.

Bourk, T.R. (1976) Electrical Responses of Neural Units in Anteroventral Cochlear Nucleus of the Cat (Ph.D. dissertation). Cambridge, MA: Massachusetts Institute of Technology, Department of Electrical Engineering.

Bourk, T.R., J.P. Mielcarz, and B.E. Norris (1981) Tonotopic organization of the anteroventral cochlear nucleus of the cat. Hear. Res. *4:*215–241.

Brawer, J.R., D.K. Morest, and E.C. Kane (1974) The neuronal architecture of the cochlear nucleus of the cat. J. Comp. Neurol. *155:*251–300.

Brown, M.C., A.M. Berglund, N.Y.-S. Kiang, and D.K. Ryugo (1988a) Central trajectories of type II spiral ganglion neurons. J. Comp. Neurol. *278:*581–590.

Brown, M.C., M.C. Liberman, T.E. Benson, and D.K. Ryugo (1988b) Brainstem branches from olivocochlear axons in cats and rodents. J. Comp. Neurol. *278:*591–603.

Brown, M.C., and J.V. Ledwith (1990) Projections of thin (type-II) and thick (type-I) auditory-nerve fibers into the cochlear nucleus of the mouse. Hear. Res. *49:*105–118.

Burian, M., and W. Goesttner (1988) Projection of primary vestibular afferent fibers to the cochlear nucleus in the guinea pig. Neurosci. Lett. *84:*13–17.

Caicedo, A., and H. Herbert (1993) Topography of descending projections from the inferior colliculus to auditory brainstem nuclei in the rat. J. Comp. Neurol. *328:*377–392.

Cant, N.B., and D.K. Morest (1978) Axons from non-cochlear sources in the anteroventral cochlear nucleus of the cat. A study with the rapid Golgi method. Neuroscience *3:*1003–1029.

Cant, N.B., and D.K. Morest (1979) Organization of the neurons in the anterior division of the anteroventral cochlear nucleus of the cat. Light-microscopic observations. Neuroscience *4:*1909–1923.

Cant, N.B. (1981) The fine structure of two types of stellate cells in the anterior division of the anteroventral cochlear nucleus of the cat. Neuroscience *6:*2643–2655.

Cant, N.B. (1982) Identification of cell types in the anteroventral cochlear nucleus that project to the inferior colliculus. Neurosci. Lett. *32:*241–246.

Cant, N.B., and K.C. Gaston (1982) Pathways connecting the right and left cochlear nuclei. J. Comp. Neurol. *212:*313–326.

Fekete, D.M., E.M. Rouiller, M.C. Liberman, and D.K. Ryugo (1984) The central projections of intracellularly labeled auditory nerve fibers in cats. J. Comp. Neurol. *229:*432–450.

Feliciano, M., E. Saldaña, and E. Mugnaini (1995) Direct projections from the rat primary auditory neocortex to nucleus sagulum, paralemniscal regions, superior olivary complex and cochlear nuclei. Aud. Neurosci. *1:*287–308.

Feng, A.S., and M. Vater (1985) Functional organization of the cochlear nucleus of rufous horseshoe bats (*Rhinolophus rouxi*): Frequencies and internal connections are arranged in slabs. J. Comp. Neurol. *235:*529–553.

Floris, A., M. Diño, D.M. Jacobowitz, and E. Mugnaini (1994) The unipolar brush cells of the rat cerebellar cortex and cochlear nucleus are calretinin-positive: A study by light and electron microscopic immunocytochemistry. Anat. Embryol. *189:*495–520.

Friauf, E., and J. Ostwald (1988) Divergent projections of physiologically characterized rat ventral cochlear nucleus neurons as shown by intraaxonal injection of horseradish peroxidase. Exp. Brain Res. *73:*263–284.

Ghoshal, S., and D.O. Kim (1996) Marginal shell of the anteroventral cochlear nucleus: Single unit response properties in the unanesthetized decerebrate cat. Abstracts of the Nineteenth Midwinter Research Meeting of the Association for Research in Otolaryngology, p. 169.

Gonzalez, D.L., P.J. Kim, T. Pongstaporn, and D.K. Ryugo (1993) Synapses of the auditory nerve in the dorsal cochlear nucleus of the cat. Abstracts of the Sixteenth Midwinter Research Meeting of the Association for Research in Otolaryngology, p. 119.

Hackney, C.M., K.K. Osen, and J. Kolson (1990) The cochlear nuclear complex of the guinea pig. Some anatomical observations. Anat. Embryol. *182:*123–149.

Itoh, K., H. Kamiya, A. Mitani, Y. Yasui, M. Takada, and N. Mizuno (1987) Direct projections from the dorsal column nuclei and the spinal trigeminal nuclei to the cochlear nuclei in the cat. Brain Res. *400:*145–150.

Jiang, D., A.R. Palmer, and I.M. Winter (1996) The frequency extent of two-tone facilitation in onset units in the ventral cochlear nucleus. J. Neurophysiol. *75:*380–395.

Kane, E.S., and R.C. Finn (1977) Descending and intrinsic inputs to dorsal cochlear nucleus of cats: A horseradish peroxidase study. Neuroscience *2:*897–912.

Kevetter, G.A., and A.A. Perachio (1989) Projections from the sacculus to the cochlear nuclei in the Mongolian gerbil. Brain Behav. Evol. *34:*193–200.

Liberman, M.C. (1991) Central projections of auditory-nerve fibers of differing spontaneous rate. I. Anteroventral cochlear nucleus. J. Comp. Neurol. *313:*240–258.

Liberman, M.C. (1993) Central projections of auditory-nerve fibers of differing spontaneous rate, II: Posteroventral and dorsal cochlear nuclei. J. Comp. Neurol. *327:*17–36.

Lorente de Nó, R. (1933) Anatomy of the eighth nerve-III. General plans of structure of the primary cochlear nuclei. Laryngoscope *43:*327–350.

Lorente de Nó, R. (1981) The Primary Acoustic Nuclei. New York: Raven Press.

Malmierca, M.S., F.E.N. Lebeau, and A. Rees (1996) The topographical organization of descending projections from the central nucleus of the inferior colliculus in guinea pig. Hear. Res. *93:*167–180.

Mugnaini, E., K.K. Osen, A. Dahl, V.L. Friedrich Jr., and G. Korte (1980a) Fine structure of granule cells and related interneurons (termed Golgi cells) in the cochlear nuclear complex of cat, rat, and mouse. J. Neurocytol. *9:*537–570.

Mugnaini, E., B.W. Warr, and K.K. Osen (1980b) Distribution and light microscopic features of granule cells in the cochlear nuclei of cat, rat, and mouse. J. Comp. Neurol. *191:*581–606.

Nelken, I., and E.D. Young (1994) Two separate inhibitory mechanisms shape the responses of dorsal cochlear nucleus Type IV units to narrowband and wideband stimuli. J. Neurophysiol. *71:*2446–2462.

Oertel, D., S.H. Wu, M.W. Garb, and C. Dizack (1990) Morphology and physiology of cells in slice preparations of the posteroventral cochlear nucleus of mice. J. Comp. Neurol. *295:*136–154.

Osen, K.K. (1969) Cytoarchitecture of the cochlear nuclei in the cat. J. Comp. Neurol. *136:*453–484.

Osen, K.K. (1970) Course and termination of the primary afferents in the cochlear nuclei of the cat. Arch. Ital. Biol. *108:*21–51.

Osen, K.K., O.P. Ottersen, and J. Storm-Mathisen (1990) Colocalization of glycine-like and GABA-like immunoreactivities: A semiquantitative study of individual neurons in the dorsal cochlear nucleus of cat. In O.P. Ottersen and J. Storm-Mathisen (eds): Glycine Neurotransmission. New York: John Wiley & Sons, pp. 417–451.

Palmer, A.R., and I.M. Winter (1993) Best frequency (BF) threshold reductions caused by off-BF non-excitatory tones in onset units of the cochlear nucleus. Abstracts of the Sixteenth Midwinter Research Meeting of the Association for Research in Otolaryngology, p. 123.

Palmer, A.R., D. Jiang, and D.H. Marshall (1996) Responses of ventral cochlear nucleus onset and chopper units as a function of signal bandwidth. J. Neurophysiol. *75:*780–794.

Pfeiffer, R.R. (1966) Classification of response patterns of spike discharges for units in the cochlear nucleus: Tone burst stimulation. Exp. Brain Res. *1:*220–235.

Poljak, S. (1926) Untersuchungen am oktavus-system dersäugetiere und an den mit diesem koordinierten motorischen apparaten des hirnstammes. J. Physiol. Psych. Neurol. *32:*170–231.

Pont, M.J., and R.I. Damper (1991) A computational model of afferent neural activity from the cochlea to the dorsal acoustic stria. J. Acoust. Soc. Am. *89:*1213–1228.

Ramón y Cajal, S. (1909) Histologie du Système nerveux de l'Homme et des Vertébrés, Vol. 1. Madrid:Instituto Ramón y Cajal, pp. 774–838.

Rhode, W.S., and S. Greenberg (1994) Lateral suppression and inhibition in the cochlear nucleus of the cat. J. Neurophysiol. *71:*493–514.

Rhode, W.S., and P.H. Smith (1986) Encoding time and intensity in the ventral cochlear nucleus of the cat. J. Neurophysiol. *56:*262–286.

Ryugo, D.K. (1992) The auditory nerve: Peripheral innervation, cell body morphology, and central projections. In D.B. Webster, A.N. Popper, R.R. Fay (eds): The Mammalian Auditory Pathway: Neuroanatomy. New York: Springer-Verlag pp. 23–65.

Ryugo, D.K., and S.K. May (1993) The projections of intracellularly labeled auditory nerve fibers to the dorsal cochlear nucleus of cats. J. Comp. Neurol. *329:*20–35.

Ryugo, D.K., T. Pongstaporn, D.D. Wright, and A.H. Sharp (1995) Inositol 1,4,5-trisphosphate receptors: Immunocytochemical localization in the dorsal cochlear nucleus. J. Comp. Neurol. *358:*102–118.

Ryugo, D.K., F.H. Willard, and D.M. Fekete (1981) Differential afferent projections to the inferior colliculus from the cochlear nucleus in the albino mouse. Brain Res. *210:*342–349.

Ryugo, D.K., D.D. Wright, and T. Pongstaporn (1993) Ultrastructural analysis of synaptic endings of auditory nerve fibers in cats: Correlations with spontaneous discharge rate. In M.A. Merchán, Juiz, J.M., Godfrey, D.A., Mugnaini, E. (eds.): Proceedings of a NATO Advanced Research Workshop on the Mammalian Cochlear Nuclei: Organization and Function. New York: Plenum Press p. 65–74.

Schofield, B.R., and N.B. Cant (1996) Origins and targets of commissural connections between the cochlear nuclei in guinea pigs. J. Comp. Neurol. *375:*128–146.

Smith, P.H., and W.S. Rhode (1989) Structural and functional properties distinguish two types of multipolar cells in the ventral cochlear nucleus. J. Comp. Neurol. *282:*595–616.

Snyder, R.L., and P.A. Leake (1988) Intrinsic connections within and between cochlear nucleus subdivisions in cat. J. Comp. Neurol. *278:*209–225.

Spirou, G.A., and E.D. Young (1991) Organization of dorsal cochlear nucleus Type IV unit response maps and their relationship to activation by band-limited noise. J. Neurophysiol. *66:*1750–1768.

Warr, W.B. (1966) Fiber degeneration following lesions in the anteroventral cochlear nucleus of the cat. Exp. Neurol. *14:*453–474.

Weedman, D.L., T. Pongstaporn, and D.K. Ryugo (1996) Ultrastructural study of the granule cell domain of the cochlear nucleus in rats: Mossy fiber endings and their targets. J. Comp. Neurol. *369:*345–360.

Weedman, D.L., and D.K. Ryugo (1996a) Projections from auditory cortex to the cochlear nucleus in rats: Synapses on granule cell dendrites. J. Comp. Neurol. *371:*311–324.

Weedman, D.L., and D.K. Ryugo (1996b) Pyramidal cells in primary auditory cortex project to cochlear nucleus in rat. Brain Res. *706:*97–102.

Weinberg, R.J., and A. Rustioni (1987) A cunecochlear pathway in the rat. Neuroscience *20:*209–219.

Wickesberg, R.E., and D. Oertel (1988) Tonotopic projection from the dorsal to the anteroventral cochlear nucleus of mice. J. Comp. Neurol. *268:*389–399.

Winter, I.M., and A.R. Palmer (1995) Level dependence of cochlear nucleus onset unit responses and facilitation by second tones or broadband noise. J. Neurophysiol. *73:*141–159.

Wouterlood, F.G., E. Mugnaini, K.K. Osen, and A.L. Dahl (1984) Stellate neurons in rat dorsal cochlear nucleus studied with combined Golgi impregnation and electron microscopy: Synaptic connections and mutual coupling by gap junctions. J. Neurocytol. *13:*639–664.

Wright, D.D., C.D. Blackstone, R.L. Huganir, and D.K. Ryugo (1996) Immunocytochemical localization of the mGluR1α metabotropic glutamate receptor in the dorsal cochlear nucleus. J. Comp. Neurol. *364:*729–745.

Wright, D.D., and D.K. Ryugo (1996) Mossy fiber projections from the cuneate nucleus to the cochlear nucleus in the rat. J. Comp. Neurol. *365:*159–172.

Young, E.D., and W.E. Brownell (1976) Responses to tones and noise of single cells in dorsal cochlear nucleus of unanesthetized cats. J. Neurophysiol. *39:*282–300.

Young, E.D., I. Nelken, and R.A. Conley (1995) Somatosensory effects on neurons in dorsal cochlear nucleus. J. Neurophysiol. *73:*743–765.

Young, E.D., J.M. Robert, and W.P. Shofner (1988) Regularity and latency of units in ventral cochlear nucleus: Implications for unit classification and generation of response properties. J. Neurophysiol. *60:*1–29.

Zhang, S., and D. Oertel (1993a) Giant cells of the dorsal cochlear nucleus of mice: Intracellular recordings in slices. J. Neurophysiol. *69:*1398–1408.

Zhang, S., and D. Oertel (1993b) Tuberculoventral cells of the dorsal cochlear nucleus of mice: Intracellular recordings in slices. J. Neurophysiol. *69:*1409–1421.